Archives of Environmental Protection
Vol. 49 no. 1 pp. 47–56

PL ISSN 2083-4772
DOI 10.24425/aep.2023.144736



# Removal of Direct Orange 26 azo dye from water using natural carbonaceous materials

Krzysztof Kuśmierek[1], Lidia Dąbek[2]*, Andrzej Świątkowski[1]

[1]Institute of Chemistry, Military University of Technology, Warsaw, Poland
[2]Faculty of Environmental Engineering, Geomatics and Renewable Energy, Kielce University of Technology, Poland

*Corresponding author's e-mail: ldabek@tu.kielce.pl

**Keywords:** adsorption, lignite, hard coal, peat, Direct Orange 26

**Abstract:** The aim of the study was to assess the possibility of using natural carbonaceous materials such as peat, lignite, and hard coal as low-cost sorbents for the removal of Direct Orange 26 azo dye from an aqueous solution. The adsorption kinetics and the influence of experimental conditions were investigated. The following materials were used in the research: azo dye Direct Orange 26, Spill-Sorb "Fison" peat (Alberta, Canada), lignite (Bełchatów, Poland), and hard coal ("Zofiówka" mine, Poland). The morphology and porous structure of the absorbents were tested. Dye sorption was carried out under static conditions, with different doses of sorbents, pH of the solution, and ionic strength. It was observed that the adsorption of Direct Orange 26 dye on all three adsorbents was strongly dependent on the pH of the solution, while the ionic strength of the solution did not affect the adsorption efficiency. The adsorption kinetics were consistent with the pseudo-second-order reaction model. The stage which determines the rate of adsorption is the diffusion of the dye in the near-surface layer. The process of equilibrium adsorption of Direct Orange 26 dye on all tested adsorbents is best described by the Langmuir isotherm. The maximum adsorption capacity for peat, brown coal and hard coal was 17.7, 15.1 and 13.8 mg/g, respectively. The results indicate that peat, lignite, and hard coal can be considered as alternative adsorbents for removing azo dyes from aqueous solutions.

## Introduction

Wastewater dyes from the textile, paper, tanning, distillery, food industries and the production of dyes itself pose a significant threat to the environment. Despite the huge production volume, exact data on the number of dyes released into the environment are not available. It is estimated that about 10–15% of the dyes used end up in the environment along with sewage. At the same time, it is known that these substances are highly toxic, mutagenic, and low biodegradable (Wani et al. 2020). They are extremely harmful to living organisms, they can cause allergies, and skin sensitization, which often leads to neoplastic diseases. When discharged into water, they negatively affect the processes of photosynthesis, disrupt the transmission of light, and disturb the biocenosis in the ecosystem (Lellis et al. 2019).

Because of the significant threat posed by dyes to the aquatic environment, an extremely important problem is the effective and efficient treatment of wastewater containing these pollutants. Due to the complex chemical structure and physical and chemical properties of substances used as dyes, the selection of an effective method of their removal is a complex and difficult problem, which is still the subject of numerous studies. Currently, the most commonly used methods are adsorption, coagulation, oxidation, and ultrafiltration. It should be noted that the use of chemical methods of removing dyes from wastewater is associated with the problem of the formation of intermediate products of decomposition of these substances (with equally toxic properties), as well as with the formation of significant amounts of sewage sludge. Therefore, an alternative and frequently used solution is adsorption. Due to the wide range of sorbents, selectivity, easy implementation of the process, low operating costs, and the lack of onerous sewage sludge formation, this method is increasingly used.

A significant limitation of the use of this process is the high costs of obtaining and regenerating the most used sorbents, such as activated carbons or zeolites. For this reason, there is need and justified research on the search for new adsorbents with a satisfactory sorption capacity, preferably classified as low-cost sorbents, i.e., materials that do not require additional processing, are of natural origin, or are waste requiring disposal, are safe for the environment, and available in significant amounts (Gupta & Suhas 2009, Sočo et al. 2020). Among natural substances with the characteristics of sorbents that can be used as dye sorbents, peat, lignite, and hard coal are of significant importance (Venkata Mohan et al. 2002, Sepulveda et al. 2004, Rusu et al. 2014, Dzieniszewska and Kyzioł-Komosińska 2018). These raw materials differ in the

degree of metamorphism, carbonization, and, consequently, different physical and chemical properties as well as their porous structure and sorption capacity (O'Keefe et al. 2013).

Peat is an organogenic sedimentary rock and a product of the first stage of plant carbonization. It is common in Europe, Asia, and North America. This sedimentary rock has the lowest carbon content (<60%) and a high moisture content (75%) and volatile matter (>60%). Currently, peat is used both as fuel and for fertilization in agriculture and horticulture, as well as for medical and sanitary purposes. The sorption properties of peat result from the presence of fulvic and humic acids, and consequently the presence of the –COOH and –OH functional groups, which determine the ion-exchange properties of this material.

Lignite has a carbon content of approximately 70%, moisture content of 30%, and volatile matter content of over 50%. The use of lignite as sorbent results from both its developed porous structure and the chemical structure of the surface. In its structure, it contains functional groups (carboxyl, phenolic hydroxyl, and carbonyl) responsible for high cation exchange capacity. These properties are used to remove inorganic and organic compounds, including dyes.

A significant advantage of peat and lignite resulting from their chemical composition and structure is the possibility of using these materials in the soil and water environment, both to restore humic substances in the topsoil and bind impurities, as well as fill sorption barriers or as additives to natural sorption barriers and as sleeve fillings for isolating pollution foci. However, this application requires thorough research in the field of the evaluation of sorption capacity in relation to selected groups of pollutants and understanding the mechanisms and kinetics of binding individual groups of pollutants on the surface of these sorbents, which justifies research in this area.

Among the natural carbon resources mentioned above, hard coal is material with the highest carbon and volatile matter content and the lowest moisture content. It is mainly used as an energy raw material, as well as a raw material for the production of activated carbons. Nevertheless, due to the extensive porous structure and the presence of the following functional groups: hydroxyl, carboxyl, carbonyl, methoxy, and ether, it also has sorption capacity, in particular concerning vapor and gas sorption (Kreiner and Żyła 2006). The adsorption of gases ($CO_2$, methane, water vapor, hydrocarbons, etc.) on hard coal has been widely researched and well documented in the literature, while little is known about the behavior of hard coal as an adsorbent for pollutants from aqueous solutions. Few studies describe the use of coal as a cheap adsorbent for sorption from water solutions, e.g., for removing metal ions, dyes, chlorobenzene, nitrobenzene, phenol, and chlorophenol (Tarasevich 2002, Kuśmierek et al. 2016). These works show that hard coal can be used as a sorbent for pollutants in the aquatic environment. For this reason, it is justified to continue research in this area.

In works devoted to the adsorption of dyes on natural carbon materials, generally one carbon material was used for research, e.g., peat, lignite or hard coal. In individual works, one dye was usually used, different in each work (Allen et al. 2004, Hassani et al. 2014, de Mattos et al. 2019). This made it impossible to make any comparisons. A novelty in our work is the use of three natural carbon materials and the adsorption of the same dye on them.

The presented study aimed to compare the sorption capacity of natural carbon materials with different levels of metamorphism, such as peat (PT), lignite (BC), and hard coal (HC), against a selected representative of the azo dyes group – Direct Orange 26, depending on the process conditions. The selected compound belongs to one of the most important groups of dyes (azo dyes), which constitute a significant part of the global production of synthetic dyes.

## Experimental

### *Chemicals and materials*

The azo dye Direct Orange 26 (DO26, CAS Number: 3626-36-6), the structural formula of which is shown in Fig. 1, was received from Boruta-Zachem SA (Bydgoszcz, Poland). Other high-purity reagents were purchased from Chempur (Piekary Śląskie). Commercially available Spill-Sorb "Fison" peat from the Parland County peat bog (Alberta, Canada), brown coal from the Bełchatow (Poland) deposit, and hard coal from the "Zofiówka" mine (Poland) were used as adsorbents. The raw adsorbent samples were crushed in a mortar, sieved to obtain a homogeneous fraction, washed with distilled water, and dried at 120°C for 24 h.

### *Adsorbents characterization*

The study of the surface morphology of the peat, lignite, and hard coal samples was carried out with the use of a desktop scanning electron microscope Phenom XL Thermo Fisher Scientific, Nanoscience Instruments. The EDS analyzer of the BDD type, with which the scanning electron microscope was equipped, was used to determine the chemical composition of the surface of the tested samples.

The porosity of all materials was characterized by low-temperature (77 K) $N_2$ adsorption-desorption isotherms determined with the use of the ASAP 2020 volumetric adsorption analyzer (Micromeritics, Norcross, GA, USA). Before each adsorption measurement, the samples were degassed at 120°C under a vacuum.

The point of zero charge ($pH_{PZC}$) of the natural carbonaceous materials was determined by the following procedure. Solutions of 0.1 mol/L sodium chloride (20 mL) were adjusted to an appropriate pH ranging from 2 to 12 by the addition of small amounts of 0.1 mol/L NaOH and/or 0.1 mol/L HCl. Then, 0.05 g of adsorbent was added to the solutions. The mixtures were then shaken for 24 h, filtered through filter paper and the pH of the solutions was measured. The final pH was plotted against the initial pH and the intersection point of the obtained curve was taken as the $pH_{PZC}$.

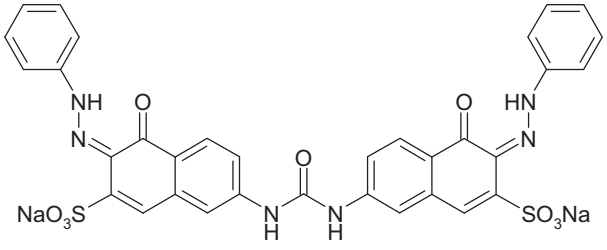


**Fig. 1.** The structural formula of the Direct Orange 26 dye molecule

### *Adsorption experiments*

All adsorption experiments were conducted at 25°C in Erlenmeyer flasks containing 20 mL of DO26 solutions at various concentrations (from 20 to 100 µmol/L). After adding the appropriate amount of adsorbent to the solutions, the flasks were shaken at 100 rpm. After sufficient time (kinetic studies) or after 8 h, the solutions were filtered through filter paper and analyzed for dye content. The dye concentration of the solutions was determined spectrophotometrically using a Carry 3E spectrophotometer (Varian, USA) at an analytical wavelength of λ = 492 nm. The calibration curve obtained showed a straight-line character over the concentration range tested (from 5 to 80 µmol/L) with a high $R^2$ value (0.999) and was described by the equation: $y = 0.0198x + 0.0037$. The adsorption amount per mass of adsorbent was calculated using the following equations:

$$q_t = \frac{(C_0 - C_t)V}{m} \quad (1)$$

$$q_e = \frac{(C_0 - C_e)V}{m} \quad (2)$$

where: $q_e$ – adsorption at equilibrium conditions (µmol/g); $q_t$ – adsorption after time $t$ (µmol/g); $C_0$ – initial dye concentration (µmol/L); $C_e$ – equilibrium concentration of the dye (µmol/L); $V$ – solution volume (L); $m$ – adsorbent mass (g).

The removal efficiency of DO26 on the peat, lignite, and hard coal was evaluated using the following equation:

$$\text{Removal } \% = \frac{(C_0 - C_e)}{C_0} \times 100 \quad (3)$$

The effect of the initial adsorbent dose, as well as the effects of solution pH and ionic strength, were investigated. These experiments as well as kinetic studies were conducted for an initial dye concentration of 50 µmol/L. The natural (original) pH of the dye solution (pH ~ 7.4) was selected for the adsorption studies. Kinetics, as well as pH, and ionic strength experiments, were carried out for an adsorbent mass of 0.05 g (2.5 g/L). All experiments were repeated twice and the averaged value was taken for calculations.

## Results and discussion

### *Characterization of adsorbents*

The received SEM images of peat, lignite, and hard coal are shown in Fig. 2. The shape of grains of the tested materials and their outer surface show significant differences. Comparing the peat, lignite, and hard coal SEM images at magnification 300× (Fig. 2 a, b, c), one can observe an increasingly smooth surface in this order and more and more angular shape of their grains. The SEM images for a magnification of 1,500× show the surface structure of peat, lignite, and hard coal grains. One can observe in this order (increasing degree of metamorphism) a fibrous, fine-fibrous, and fine-crystalline structure.

The obtained results of the determined chemical composition of the surface of peat, lignite, and hard coal are presented in Table 1. As can be seen, the carbon content increases with the degree of metamorphism of these samples. The relatively high oxygen content decreases but varies relatively little. The nitrogen content drops significantly. Likewise, the calcium content drops quickly and for hard coal, it is no longer observed. The contents of other elements are already very low (below 1%) and only for lignite – slightly more than 5 wt.% of boron is observed.

Nitrogen adsorption isotherms for the peat, lignite, and hard coal samples are presented in Fig. 3. All of these three curves can be classified as type II adsorption isotherms according to the Brunauer classification (Bansal and Goyal 2005). The specific surface areas of the materials were calculated using the Brunauer-Emmett-Teller equation and

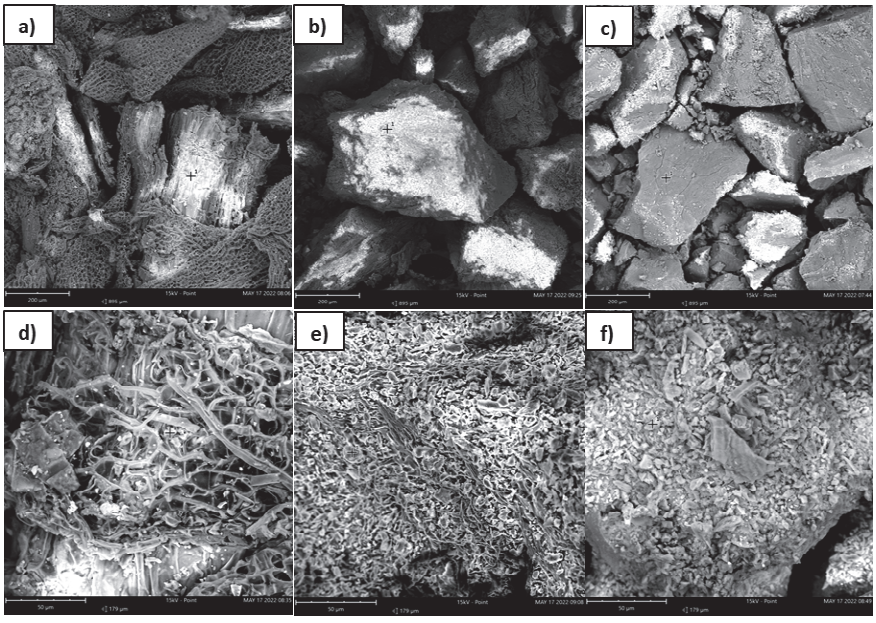


**Fig. 2.** The SEM images of (a, d) peat, (b, e) lignite, and (c, f) hard coal external surfaces. Magnification 300× (a–c) and magnification 1,500× (d–f)

were found to be 0.4 $m^2/g$ for hard coal, 1.2 $m^2/g$ for lignite, and 9.1 $m^2/g$ for peat. The total pore volumes ($V_t$) were in turn equal to 0.00071 $cm^3/g$, 0.00224 $cm^3/g$ and 0.0247 $cm^3/g$ for these materials, respectively.

### *Effect of adsorbent dose*

In the first step, the effect of initial adsorbent mass on adsorption was checked. The experiments were carried out for three different amounts of adsorbent: 20, 50, and 100 mg, respectively, which corresponded to adsorbent doses of 1; 2.5, and 5 g/L. The results are shown in Fig. 4.

As the adsorbent dose increased from 1 g/L to 5 g/L, the dye removal efficiency increased from 38 to 71% for HC, from 41 to 77% for BC, and from 55 to 92% for PT, respectively. The observed increase in adsorption efficiency with increasing adsorbent dose can be explained by the higher amount and greater availability of active adsorption sites available to the adsorbate molecules. A much more marked increase in adsorption efficiency was observed when increasing the adsorbent dose from 1 to 2.5 g/L than from 2.5 to 5 g/L. For example, increasing peat dose from 1 to 2.5 g/L increased DO26 removal efficiency from 38 to 61% (an increase of 23 percentage points), while increasing peat from 2.5 to 5 g/L increased adsorption efficiency by only 10 percentage points (from 61 to 71%). A similar trend was also observed for lignite and hard coal. Such a phenomenon suggests that adding too much adsorbent is not beneficial. Too much adsorbent dose causes, among other things, deposition of adsorbent particles on the inner walls of the flask and difficult mixing of the mixture, leading to a much lower increase in adsorption efficiency than would be expected. Therefore, 50 mg (2.5 g/L) of adsorbent was considered to be the optimum adsorbent amount. An increase in adsorption efficiency with increasing adsorbent dosage has also been reported in other articles, e.g., for the adsorption of DO26 on sawdust (Izadyar and Rahimi 2007, Kuśmierek et al. 2020a) and rice husk (Safa and Bhatti 2011).

### *Effects of solution pH and ionic strength*

The physicochemical properties of adsorbent and adsorbate as well as properties of the solution including its pH and the presence of inorganic salts (ionic strength), play an important role in the adsorption process. The effect of solution pH on the adsorption efficiency of DO26 was investigated in the pH range from 2.5 to 11.0 and the results are presented in Fig. 5a. The results showed a strong pH dependence of dye adsorption on all three adsorbents. Adsorption occurred best in an acidic medium (pH = 2.5) and successively decreased with increasing pH. The increase in solution pH from 2.5 to 11 resulted in a decrease in DO26 removal from 81 to 40% on PT, from 77 to 23% on BC, and from 76 to 10% on HC, respectively.

The structural formula of DO26 is shown in Fig. 1. As can be seen, Direct Orange 26 is an anionic dye with sulfonic acid groups ($R\text{-}SO_3Na$) in the molecule, which exists in dissociated form ($R\text{-}SO_3^-$) in an aqueous solution. The determined zero charge points of the adsorbents were 6.05, 6.45, and 6.65 for PT, BC, and HC, respectively. These values give information about the type of charge present on the adsorbent surface. Thus, in a solution with pH below $pH_{PZC}$, a positive charge accumulates on the adsorbent surface, while in a solution with pH above $pH_{PZC}$, the adsorbent surface is negatively charged. Therefore, the highest adsorption capacity values recorded at pH 2.5 are due to the attractive electrostatic force between the positively charged adsorbent surface and the negatively charged DO26 molecules. As the pH of the solution increases,

**Table 1.** The EDS analysis for the peat, lignite, and hard coal samples (wt.%)

| Carbon materials | C | O | N | Ca | B | S | K | Si | Al |
|---|---|---|---|---|---|---|---|---|---|
| Peat | 49.50 | 33.57 | 8.52 | 2.74 | 5.10 | 0.32 | 0.16 | 0.09 | – |
| Lignite | 61.02 | 31.30 | 6.41 | 0.59 | – | 0.53 | – | 0.06 | 0.09 |
| Hard coal | 70.12 | 28.04 | 1.25 | – | – | 0.51 | – | – | 0.08 |

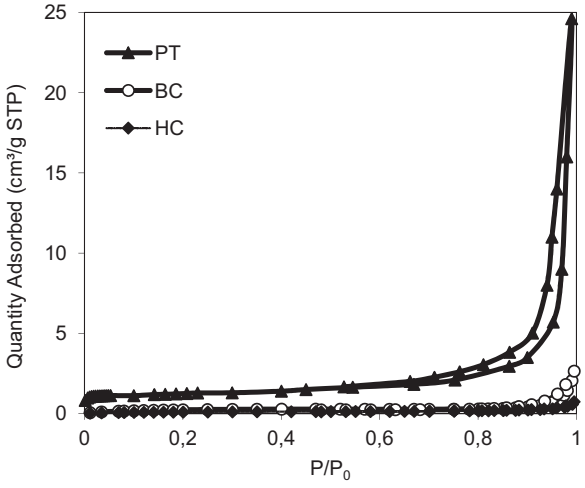


**Fig. 3.** Nitrogen adsorption isotherms for the peat, lignite, and hard coal samples

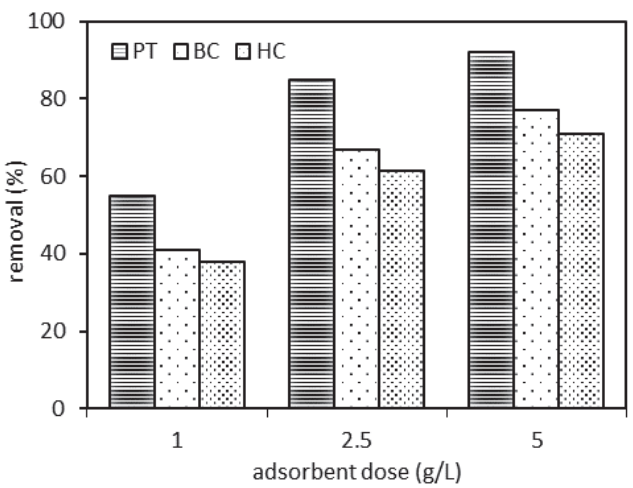


**Fig. 4.** Effect of adsorbent dose on the adsorption of DO26 dye on the peat, lignite, and hard coal

the number of positively charged sites on the adsorbent surface decreases, and thus the number of negatively charged sites increases. As a result, there is a successive decrease in adsorption efficiency due to the repulsive electrostatic force between the negatively charged adsorbent surface and the dye anion. Similar adsorption behavior of DO26 with a variation in the solution pH was reported on the rice husk (Safa and Bhatti 2011), sawdust (Kuśmierek et al. 2020a), Fe@graphite composite (Konicki et al. 2017), and halloysites (Kuśmierek et al. 2020b).

The removal of dyes from aqueous solutions by various adsorbents is a very complex and sophisticated process. Specific adsorption mechanisms include physical adsorption, ion exchange, electrostatic interactions, and surface complexation (Goswami et al. 2022). The concept of $pH_{PZC}$ seems to explain well the adsorption behavior of the dye on the materials tested. This suggests that electrostatic interactions (attractive and/or repulsive) are one of the prime adsorption mechanisms for the adsorption of DO26 dye on these natural carbonaceous materials. Of course, as mentioned earlier, the process is more complex and various other mechanisms may be involved in the adsorption process (e.g. physical interactions such as pore filling, stacking, and H-bonding). Thus, it can be assumed that the adsorption of DO26 on peat, lignite and hard coal takes place mainly through electrostatic adsorbent-adsorbate interactions but also (simultaneously) *via* hydrogen bonding and π-π interactions.

The adsorption of DO26 from solutions containing different concentrations of sodium sulfate (0.01, 0.05, and 0.1 mol/L) was also investigated in this study. The effect of the ionic strength of the solution on the adsorption of the dye is shown in Fig. 5b. As can be seen, increasing the salt concentration in the solution (increasing the ionic strength) did not affect the adsorption efficiency of DO26 on used carbonaceous materials. A similar regularity, no apparent effect of solution ionic strength on DO26 adsorption, was reported for halloysites (Kuśmierek et al. 2020b).

### *Adsorption kinetics*

The adsorption rate of DO26 dye on all three materials is shown in Fig. 6. The adsorption equilibrium was established after about 30 min. Two most popular kinetic models including

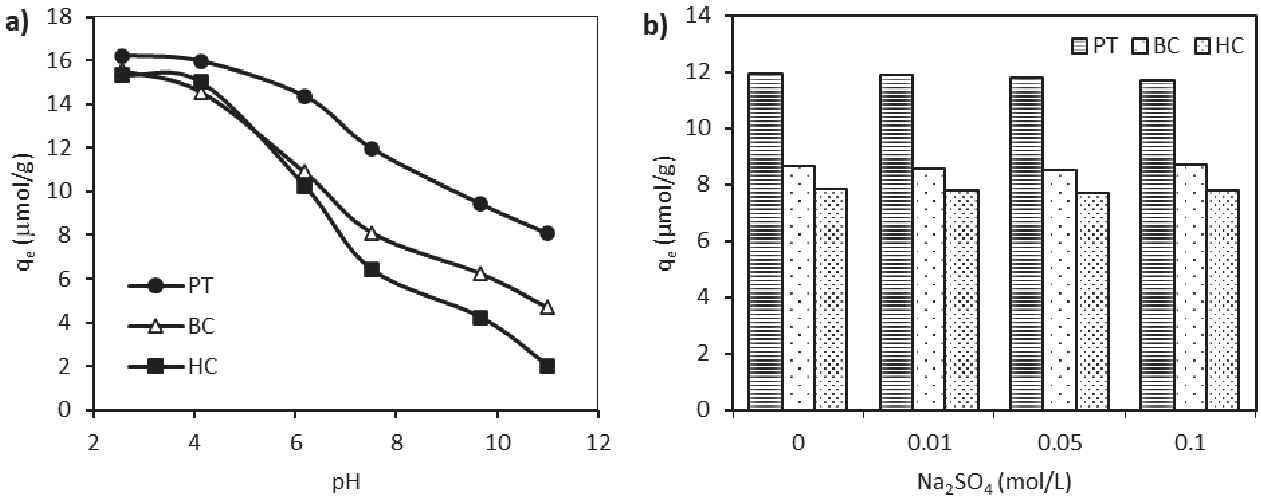


**Fig. 5.** Effects of solution pH (a) and ionic strength (b) on the adsorption of DO26 on the peat, lignite, and hard coal

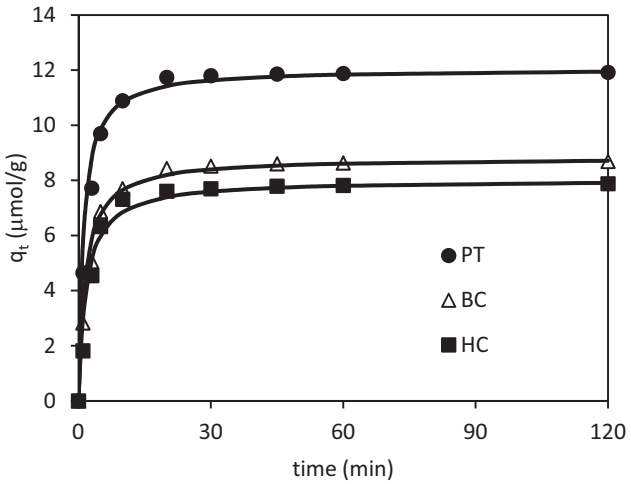


**Fig. 6.** Adsorption kinetics of DO26 on the tested materials (line – fitting of pseudo-second-order kinetic model)

pseudo-first-order (PFO) and pseudo-second-order (PSO) were used to describe the adsorption process (Tan and Hameed 2017, Kajjumba et al. 2018). The PFO (4) and PSO (5) equations are expressed as:

$$\log(q_e - q_t) = \log q_e - \frac{k_1}{2.303} t \quad (4)$$

$$\frac{t}{q_t} = \frac{1}{k_2 q_e^2} + \frac{1}{q_e} t \quad (5)$$

where $k_1$ and $k_2$ are the PFO (1/min) and the PSO rate constants (g/µmol·min), respectively.

The values of adsorption rate constants and correlation coefficients were determined using the linear regression method and the obtained results are shown in Table 2.

As can be seen, significantly higher $R^2$ values (≥0.999) were obtained for the PSO equation. Also, a higher agreement of $q_{e\,CAL}$ with the experimental value of $q_{e\,EXP}$ was obtained for the PSO model. This shows that the adsorption kinetics of the DO26 on all three materials follows the pseudo-second-order model. No clear differences were observed in the adsorption rate of DO26 on these adsorbents; the obtained $k_2$ values for PT, BC, and HC were almost identical (0.073, 0.074, and 0.072 g/µmol·min, respectively).

Similar findings, a better fit of the pseudo-second-order model to experimental data, were reported by other authors when adsorbing DO26 onto rice husk (Safa and Bhatti 2011, Safa et al. 2011), Fe@graphite core-shell nanocomposite (Konicki et al. 2017), oak sawdust (Kuśmierek et al. 2020a) and halloysites (Kuśmierek et al. 2020b). On the other hand, Izadyar and Rahimi (2007) reported that the uptake of DO26 from aqueous solution by beechwood sawdust followed first-order kinetics.

Adsorption from solution is a multi-step process involving: (i) film diffusion, (ii) intra-particle diffusion, and (iii) adsorption, that is, localization of adsorbate molecules on the active sites of the adsorbent surface (Tan and Hameed 2017). The rate of adsorption is determined by the slowest processes, i.e., either film diffusion or intra-particle diffusion, or both. The identification of the step that determines the entire process is enabled by the Weber-Morris and Boyd models (Tan and Hameed 2017, Kajjumba et al. 2018). The Weber-Morris (intra-particle diffusion) model is given by the following equation:

$$q_t = k_i t^{0,5} + C_i \quad (6)$$

where $k_i$ is the intra-particle diffusion rate constant (µmol/g min$^{-0.5}$), and $C_i$ is the thickness of the boundary layer.

The Boyd equation is expressed as:

$$\frac{q_t}{q_e} = 1 - \frac{6}{\pi^2} \sum_1^\infty \left(\frac{1}{n^2}\right) \exp(-n^2 B_T) \quad (7)$$

where $B_T$ is a mathematical function of $q_t/q_e$.

The $B_T$ values at different contact times can be calculated using Eq. (8) (in the case of $q_t/q_e < 0.85$) and Eq. (9) (in the case of $q_t/q_e > 0.85$):

$$B_T = \pi \left(1 - \sqrt{1 - \frac{\pi}{3}\frac{q_t}{q_e}}\right)^2 \quad (8)$$

$$B_T = -0.4977 - \ln\left(1 - \frac{q_t}{q_e}\right) \quad (9)$$

Both models are shown in Fig. 7 as a plot of $q_t$ vs $t^{0.5}$ (Weber-Morris) and as a plot of $B_T$ vs $t$ (Boyd). The Weber-Morris model assumes that if the plot of $q_t = f(t^{0.5})$ is straight-line and the curve passes through the origin then adsorption is controlled only by intra-particle diffusion. A broken line in the graph (non-linearity) indicates that several processes are involved in the adsorption process and not only intra-particle diffusion. As can be seen in Fig. 7a, none of the curves passed through the origin, moreover, the dependence of $q_t$ vs $t^{0.5}$ over the whole time was not linear. This suggests that intra-particle diffusion is not the only limiting step and that the adsorption rate depends on more than just intra-particle diffusion. The Boyd model assumes that if the plot of $B_T = f(t)$ is not linear and does not pass through the origin, then the film diffusion is the most important rate-controlling step. In contrast, if the Boyd graph is a straight line and passes through the origin, then adsorption is controlled by the intra-particle diffusion step. From Boyd's plot (Fig. 7b), it can be noted that the curves are all nonlinear and do not pass through the

**Table 2.** Kinetic parameters of pseudo-first-order and pseudo-second-order models describing the adsorption kinetics of Direct Orange 26 dye on peat, lignite, and hard coal

| Parameter | Adsorbent | | |
|---|---|---|---|
| | PT | BC | HC |
| $q_{e\,EXP}$ (µmol/g) | 11.92 | 8.630 | 7.880 |
| PFO | | | |
| $q_{e\,CAL1}$ (µmol/g) | 5.341 | 4.708 | 3.145 |
| $k_1$ (1/min) | 0.108 | 0.123 | 0.078 |
| $R^2$ | 0.962 | 0.950 | 0.908 |
| PSO | | | |
| $q_{e\,CAL2}$ (µmol/g) | 12.06 | 8.826 | 7.997 |
| $k_2$ (g/µmol·min) | 0.073 | 0.074 | 0.071 |
| $R^2$ | 0.999 | 0.999 | 0.999 |

origin. These findings suggest that the adsorption of DO26 dye on peat, lignite, and hard coal is a film-diffusion mechanism.

### *Adsorption isotherms*

Adsorption isotherm experiments were carried out for constant solution volume and adsorbent dose but for different initial dye concentrations (from 20 to 100 µmol/L). The effect of initial dye concentration on its removal efficiency is shown in Fig. 8a. As can be seen, the percentage of DO26 removal decreased as the initial adsorbate concentration increased. As the initial dye concentration increased from 20 µmol/L to 100 µmol/L, the dye removal efficiency decreased from 67 to 43% for HC, from 53 to 33% for BC, and from 46 to 28% for PT, respectively.

The dependence of the amount of adsorbed DO26 dye on its equilibrium concentration in solution ($q_e = f(C_e)$) for peat, lignite, and hard coal is shown in Fig. 8b. To describe the experimental isotherms, the Freundlich (10), Langmuir (11), and Temkin (12) equations were applied (Al-Ghouti and Da'ana 2020):

$$\ln q_e = \ln K_F + \frac{1}{n} \ln C_e \tag{10}$$

$$\frac{C_e}{q_e} = \frac{1}{q_m} C_e + \frac{1}{q_m b} \tag{11}$$

$$q_e = \frac{RT}{b_T} \ln A_T + \frac{RT}{b_T} \ln C_e \tag{12}$$

where: $K_F$ ((µmol/g)(L/µmol)$^{1/n}$) and $n$ are the Freundlich isotherm constants, $q_m$ (µmol/g) and $b$ (L/µmol) are the Langmuir isotherm parameters, $b_T$ (J/mol) and $A_T$ (L/g) are the Temkin isotherm constants, $R$ is the gas constant (8.314 J/mol·K), and $T$ is the temperature (K).

The Freundlich, Langmuir, and Temkin adsorption isotherm parameters were calculated from the slope and intercept of the linear plots of $\ln q_e$ vs. $\ln C_e$, $C_e/q_e$ vs. $C_e$, and $q_e$ vs. $\ln C_e$, respectively.

The calculated parameters of the Freundlich, Langmuir and Temkin equations are shown in Table 3. By taking the $R^2$ value as the criterion for fitting the theoretical isotherm to the experimentally obtained results, it can be concluded that the sorption of DO26 dye on all three adsorbents follows the Langmuir isotherm. The Langmuir equation is based on a chemisorption model in that there are no interactions between the adsorbate molecules and the adsorbed substance forms a monolayer on the adsorbent surface. So, the good correlation with the Langmuir isotherm model suggests monolayer adsorption of the DO26 on homogeneous adsorbent surfaces.

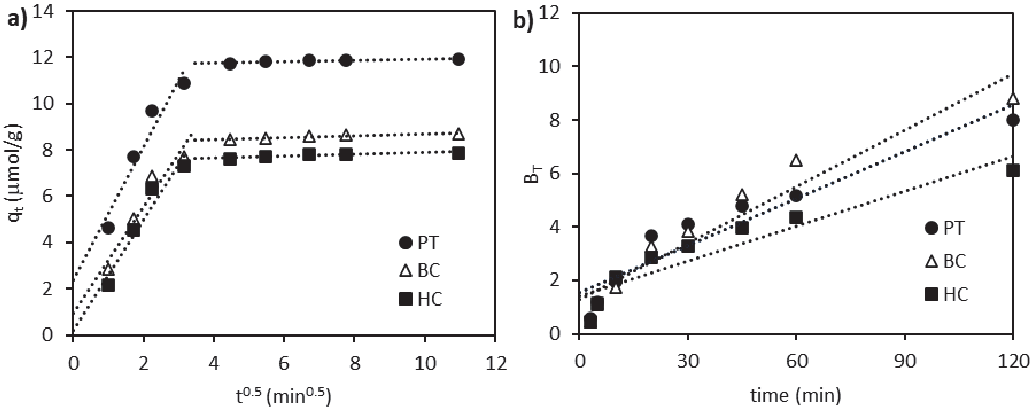


**Fig. 7.** The Weber-Morris model (a), and the plot of Boyd model (b) for the adsorption of DO26 dye onto peat, lignite, and hard coal

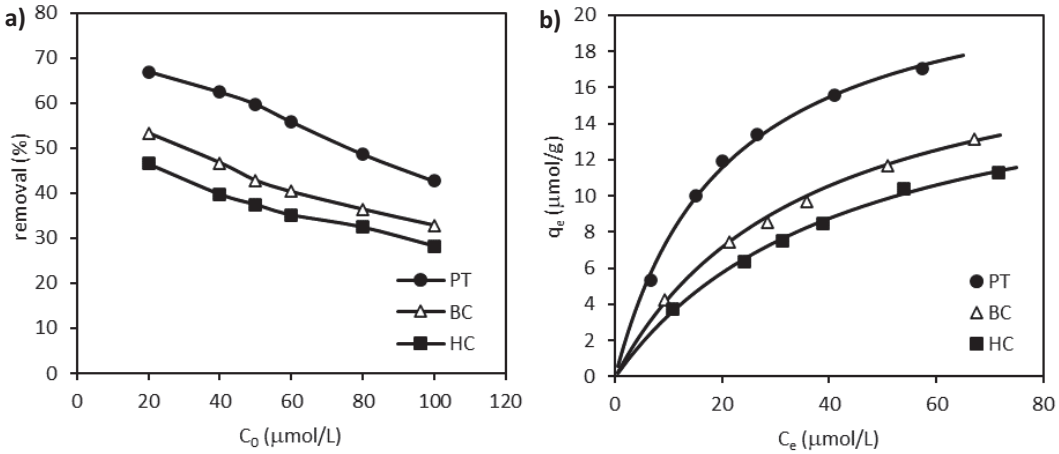


**Fig. 8.** Adsorptive removal of the DO26 dye from aqueous solutions by peat, lignite, and hard coal for their different initial concentrations at equilibrium – (a), and adsorption isotherms of DO26 from aqueous solution on PT, CB, and HC (line – fitting of Langmuir isotherm) – (b)

The DO26 dye was best adsorbed on PT (23.36 µmol/g), followed by BC (19.96 µmol/g), and least on the HC surface (18.31 µmol/g).

The evaluation of the potential suitability of used natural carbon materials as low-cost and alternative sorbents should also include a comparison of their adsorption capacity with other materials reported in the literature. The adsorption of Direct Orange 26 dye was studied on various materials including sawdust (Izadyar and Rahimi 2007, Kuśmierek et al. 2020a, Kaushik et al. 2009), rice straw (Tomczak and Tosik 2014), sugarcane bagasse pith (Kaushik et al. 2009), corn cobs (Tomczak and Blus 2016), raw and modified rice husks (Safa et al. 2011, Safa and Bhatti 2011, Bhatti et al. 2020), brick powder (Kaushik et al. 2009), magnetic Fe@graphite core-shell nanocomposite (Konicki et al. 2017), halloysites (Kuśmierek et al. 2020b), polyelectrolytes (poly(2-vinylpyridine) and poly(4-vinylpyridine)) and their composites with carbon (CarTunaF2VP and CarTunaF4VP) (Herrera-González et al. 2021) as well as copper nanoparticles synthesized from Tilapia fish scales (Rafique et al., 2022). A comparison of the adsorption capacity of the different sorbents toward DO26 is shown in Table 4.

**Table 3.** Adsorption isotherm parameters for DO26 azo dye adsorption onto peat, lignite, and hard coal

| Isotherm model | Adsorbent | | |
|---|---|---|---|
| | PT | BC | HC |
| Freundlich | | | |
| $K_F$ ((µmol/g)(L/µmol)$^{1/n}$) | 2.191 | 1.242 | 0.930 |
| $n$ | 1.878 | 1.753 | 1.671 |
| $R^2$ | 0.950 | 0.972 | 0.968 |
| Langmuir | | | |
| $q_m$ (µmol/g) | 23.36 | 19.96 | 18.31 |
| $b$ (L/µmol) | 0.049 | 0.028 | 0.023 |
| $R^2$ | 0.997 | 0.994 | 0.995 |
| Temkin | | | |
| $b_T$ (J/mol) | 453.3 | 552.1 | 604.8 |
| $A_T$ (L/g) | 0.417 | 0.257 | 0.213 |
| $R^2$ | 0.976 | 0.981 | 0.985 |

**Table 4.** Comparison of Direct Orange 26 dye adsorption on various sorbents

| Adsorbent | Adsorption capacity, $q_m$, (mg/g) | Concentration range (mg/L) | pH | Temp. | Ref. |
|---|---|---|---|---|---|
| Peat (PT) | 17.7* | 15–75 | origin | 25°C | this study |
| Lignite (BC) | 15.1* | 15–75 | origin | 25°C | this study |
| Hard coal (HC) | 13.8* | 15–75 | origin | 25°C | this study |
| beechwood sawdust | 2.78 | 20–80 | origin | – | Izadyar & Rahimi 2007 |
| oakwood sawdust | 3.73 | 15–75 | origin | 25°C | Kuśmierek et al. 2020a |
| pinewood sawdust | 3.49 | 15–75 | origin | 25°C | Kuśmierek et al. 2020a |
| cherry wood sawdust | 3.48 | 15–75 | origin | 25°C | Kuśmierek et al. 2020a |
| PVA–alginate immobilized rice husk | 16.8 | 50–200 | origin | 30°C | Safa et al. 2011 |
| raw rice husk | 19.9 | 50–200 | origin | 30°C | Safa & Bhatti 2011 |
| Fe@graphite nanocomposite | 28.3 | 5–40 | origin | 30°C | Konicki et al. 2017 |
| rye straw | 30.8 | 100–800 | 5–6 | 25°C | Tomczak & Tosik 2014 |
| carboxymethyl cellulose immobilized rice husk | 34.3 | 50–200 | origin | 30°C | Safa et al. 2011 |
| HCl-treated rice husk | 46.9 | 50–200 | origin | 30°C | Safa et al. 2011 |
| untreated halloysite | 49.1 | 15–75 | origin | 25°C | Kuśmierek et al. 2020b |
| sodium benzoate modified halloysite | 56.0 | 15–75 | origin | 25°C | Kuśmierek et al. 2020b |
| sulfuric acid-treated halloysite | 291 | 15–75 | origin | 25°C | Kuśmierek et al. 2020b |
| poly(2-vinylpyridine) polyelectrolyte | 65.8 | 250–1500 | origin | 30°C | Herrera-González et al. 2021 |
| poly(4-vinylpyridine) polyelectrolyte | 54.9 | 250–1500 | origin | 30°C | Herrera-González et al. 2021 |
| CarTunaF2VP composite | 46.1 | 250–1500 | origin | 30°C | Herrera-González et al. 2021 |
| CarTunaF4VP composite | 100 | 250–1500 | origin | 30°C | Herrera-González et al. 2021 |

* values converted from µmol/g

By comparing the values of maximum adsorption capacities in Table 4, it can be seen that peat, lignite, and hard coal can be used to remove dyes from water. Their sorption capacities are more or less comparable with other sorbents. The fossil fuels tested in this work proved to be much more effective sorbents than sawdust and comparable to raw and modified rice husks. The other sorbents presented in Table 4 had better adsorption capacity than PT, BC, and HC. However, it must be noted that the fossil fuels studied in this paper were used as adsorbents in their raw, unmodified form. The preparation of the samples for testing was limited only to crushing, sieving, and washing them with water. Additionally, all three of these adsorbents are inexpensive and readily available materials. All of this further increases their potential and applicability for removing contaminants from water.

## Conclusions

In this study, the effectiveness of three used natural carbonaceous solid materials such as peat, lignite, and hard coal in the removal of the azo dye Direct Orange 26 from the water was investigated. The adsorption kinetics and adsorption at equilibrium were studied. The equilibrium state was reached after about 30 min and the adsorption kinetics followed a pseudo-second--order kinetic model. Based on using the Weber-Morris and Boyd models one can state that the adsorption of DO26 dye on peat, lignite, and hard coal is controlled by a film-diffusion mechanism. Freundlich, Langmuir, and Temkin equations were used to describe the adsorption isotherms of DO26. The experimental results were better described by the Langmuir model. The maximum adsorption capacities for peat, lignite and hard coal were found to be 17.7, 15.1, and 13.8 mg/g, respectively. Adsorption was most effective in an acidic medium and least in a basic medium. The adsorption efficiency was not dependent on the ionic strength of the solution. The results indicate that natural carbonaceous solid materials can be used as low-cost and effective adsorbents for the removal of dyes from aqueous solutions.

## Acknowledgments

The project was funded from the program of the Minister of Science and Higher Education entitled: “Regional Initiative of Excellence” in 2019–2023 project number 025 / RID / 2018/19 financing amount PLN 12,000,000.

## References

Al-Ghouti, M.A. & Da’ana, D.A. (2020). Guidelines for the use and interpretation of adsorption isotherm models: A review. *Journal of Hazardous Materials*, 393, 122383. DOI:10.1016/j.jhazmat.2020.122383

Allen, S.J., Mckay, G. & Porter, J.F. (2004). Adsorption isotherm models for basic dye adsorption by peat in single and binary component systems. *Journal of Colloid and Interface Science*, 280, pp. 322–333. DOI:10.1016/j.jcis.2004.08.078

Bansal, R.C. & Goyal, M. (2005). Activated Carbon Adsorption, Taylor & Francis, CRC Press, Boca Raton, 2005. DOI:10.1201/9781420028812

Bhatti, H.N., Safa, Y., Yakout, S.M., Shair, O.H., Iqbal, M. & Nazir, A. (2020). Efficient removal of dyes using carboxymethyl cellulose/alginate/polyvinyl alcohol/rice husk composite: Adsorption/desorption, kinetics and recycling studies. *International Journal of Biological Macromolecules*, 150, pp. 861–870. DOI:10.1016/j.ijbiomac.2020.02.093

Dzieniszewska, A. & Kyzioł-Komosińska, J. (2018). Zdolności sorpcyjne wybranych substancji bogatych w materię organiczną w stosunku do barwników, Polska Akademia Nauk, Komitet Inżynierii Środowiska, Monografie IPIS PAN, Nr 142, Zabrze, Polska.

Goswami, L., Kushwaha, A., Kafle, S.R. & Kim, B.-S. (2022). Surface modification of biochar for dye removal from wastewater. *Catalysts*, 12, 817. DOI:10.3390/catal12080817

Gupta, V.K. & Suhas (2009). Application of low-cost adsorbents for dye removal – A review. *Journal of Environmental Management*, 90, pp. 2313–2342. DOI:10.1016/j.jenvman.2008.11.017

Hassani, A., Vafaei, F., Karaca, S. & Khataee, A.R. (2014). Adsorption of a cationic dye from aqueous solution using Turkish lignite: Kinetic, isotherm, thermodynamic studies and neural network modeling. *Journal of Industrial and Engineering Chemistry*, 20, pp. 2615–2624. DOI:10.1016/j.jiec.2013.10.049

Herrera-González, A.M., Reyes-Angeles, M.C. & Peláez-Cid, A.A. (2021). Adsorption of anionic dyes using composites based on basic polyelectrolytes and physically activated carbon. *Desalination and Water Treatment*, 230, 346–358. DOI:10.5004/dwt.2021.27445

Izadyar, S. & Rahimi, M. (2007). Use of beech wood sawdust for adsorption of textile dyes. *Pakistan Journal of Biological Sciences*, 10, 2, pp. 287–293.

Kajjumba, G.W., Emik, S., Öngen, A., Özcan, H.K. & Aydın, S. (2018). Modelling of adsorption kinetic processes – errors, theory and application. [in:] *Advanced sorption process applications*, Edebali, S. (Ed), IntechOpen, Rijeka, pp. 1–19.

Kaushik, C.P., Tuteja, R., Kaushik, N. & Sharma, J.K. (2009). Minimization of organic chemical load in direct dyes effluent using low cost adsorbents. *Chemical Engineering Journal*, 155, pp. 234–240. DOI:10.1016/j.cej.2009.07.042

Konicki, W., Hełminiak, A., Arabczyk, W. & Mijowska, E. (2017). Removal of anionic dyes using magnetic Fe@graphite core-shell nanocomposite as an adsorbent from aqueous solutions. *Journal of Colloid and Interface Science*, 497, pp. 155–164. DOI:10.1016/j.jcis.2017.03.008

Kreiner, K. & Żyła, M. (2006). Binarny charakter powierzchni węgla kamiennego. *Górnictwo i Geoinżynieria*, 30, 2, pp. 19–34.

Kuśmierek, K., Gałan, M., Kamiński, W. & Świątkowski, A. (2020a). Use of sawdust as a low-cost sorbent for the removal of azo dyes from water. *Przemysl Chemiczny*, 99, 2, pp. 201–205. DOI:10.15199/62.2020.2.2

Kuśmierek, K., Świątkowski, A., Wierzbicka, E. & Legocka, I. (2020b). Enhanced adsorption of Direct Orange 26 dye in aqueous solutions by modified halloysite. *Physicochemical Problems of Mineral Processing*, 56, 4, pp. 693–701. DOI:10.37190/ppmp/124544

Kuśmierek, K., Zarębska, K. & Świątkowski, A. (2016). Hard coal as a potential low-cost adsorbent for removal of 4-chlorophenol from water. *Water Science & Technology*, 73, 8, pp. 2025–2030. DOI:10.2166/wst.2016.046

Lellis, B., Fávaro-Polonio, C.Z., Pamphile, J.A. & Polonio, J.C. (2019). Effects of textile dyes on health and the environment and bioremediation potential of living organisms. *Biotechnology Research and Innovation*, 3, pp. 275–290. DOI:10.1016/j.biori.2019.09.001

de Mattos, N.R., de Oliveira, C.R., Camargo, L.G.B., da Silva, R.S.R. & Lavall, R.L. (2019). Azo dye adsorption on anthracite: a view of thermodynamics, kinetics and cosmotropic effects. *Separation and Purification Technology*, 209, pp. 806–814. DOI:10.1016/j.seppur.2018.09.027

O'Keefe, J.M.K., Bechtel, A., Christanis, K., Dai, S., DiMichele, W.A., Eble, C.F., Esterle, J.S., Mastalerz, M., Raymond, A.L., Valentim, B.V., Wagner, N.J., Ward, C.R. & Hower, J.C. (2013). On the fundamental difference between coal rank and coal type. *International Journal of Coal Geology*, 118, pp. 58–87. DOI:10.1016/j.coal.2013.08.007

Rafique, M.A., Kiran, S., Ashraf, A., Mukhtar, N., Rizwan, S., Ashraf, M. & Arshad, M.Y. (2022). Effective removal of Direct Orange 26 dye using copper nanoparticles synthesized from Tilapia fish scales. *Global NEST Journal*, 24, 2, pp. 311–1317. DOI:10.30955/gnj.004234

Rusu, L., Harja, M,. Simion, A.I., Suteu, D., Ciobanu, G. & Favier, L. (2014). Removal of Astrazone Blue from aqueous solutions onto brown peat. Equilibrium and kinetics studies. *Korean Journal of Chemical Engineering*, 31, 6, pp. 1008–1015. DOI:10.1007/s11814-014-0009-3

Safa, Y. & Bhatti, H.N. (2011). Kinetic and thermodynamic modeling for the removal of Direct Red-31 and Direct Orange-26 dyes from aqueous solutions by rice husk. *Desalination*, 272, pp. 313–322. DOI:10.1016/j.desal.2011.01.040

Safa, Y., Bhatti, H.N., Bhatti, I.A. & Asgher, M. (2011). Removal of Direct Red-31 and Direct Orange-26 by low cost rice husk: Influence of immobilisation and pretreatments. *Canadian Journal of Chemical Engineering*, 89, pp. 1554–1565. DOI:10.1002/cjce.20473

Sepulveda, L., Fernandez, K., Contreras, E. & Palma, C. (2004). Adsorption of dyes using peat: equilibrium and kinetic studies. *Environmental Technology*, 25, pp. 987–996. DOI:10.1080/09593332508618390

Sočo, E., Pająk, D. & Kalembkiewicz, J. (2020). Multi-component sorption and utilization of solid waste to simultaneous removing basic dye and heavy metal from aqueous system. *Archives of Environmental Protection*, 46, pp. 62–75. DOI:10.24425/aep.2020.132527

Tan, K.L. & Hameed, B.H. (2017). Insight into the adsorption kinetics models for the removal of contaminants from aqueous solutions. *Journal of the Taiwan Institute of Chemical Engineers*, 74, pp. 25–48. DOI:10.1016/j.jtice.2017.01.024

Tarasevich, Y.I. (2001). Porous structure and adsorption properties of natural porous coal. *Colloids and Surfaces A: Physicochemical and Engineering Aspects*, 176, pp. 267–272. DOI:10.1016/S0927-7757(00)00702-0

Tomczak, E. & Blus, M. (2016). Sorption dynamics of Direct Orange 26 dye onto a corncob plant sorbent. *Ecological Chemistry and Engineering S*, 23, 1, pp. 175–185. DOI:10.1515/eces-2016-0012

Tomczak, E. & Tosik, P. (2014). Sorption equilibrium of azo dyes Direct Orange 26 and Reactive Blue 81 onto a cheap plant sorbent. *Ecological Chemistry and Engineering S*, 21, 3, pp. 435–445. DOI:10.2478/eces-2014-0032

Venkata Mohan, S., Chandrasekhar Rao, N. & Karthikeyan, J. (2002). Adsorptive removal of direct azo dye from aqueous phase onto coal based sorbents: a kinetic and mechanistic study. *Journal of Hazardous Materials*, B90, pp. 189–204. DOI:10.1016/S0304-3894(01)00348-X

Wani, K.A., Jangid, N.K. & Bhat, A.R. (2020), Impact of textile dyes on public health and the environment, IGI Global, Hershey, USA.

## Wykorzystanie naturalnych materiałów węglowych do w usuwaniu barwnika azowego Direct Orange 26 z roztworu wodnego

**Streszczenie:** Celem pracy była ocena możliwości wykorzystania naturalnych materiałów węglowych takich jak torf, węgiel brunatny i węgiel kamienny jako niskokosztowych sorbentów do w usuwaniu barwnika azowego Direct Orange 26 z roztworu wodnego. Zbadano kinetykę adsorpcji oraz wpływ dawki sorbentu, pH roztworu oraz siły jonowej na skuteczność sorpcji. W badaniach wykorzystano barwnik azowy Direct Orange 26, torf Spill-Sorb „Fison" (Alberta, Kanada), węgiel brunatny (Bełchatów,Polska) oraz węgiel kamienny („Zofiówka", Polska). Wykonano badania morfologii oraz struktury porowatej absorbentów. Sorpcję barwnika prowadzono w warunkach statycznych, przy różnych dawkach sorbentów, pH roztworu i sile jonowej. Zaobserwowano, że adsorpcja barwnika Direct Orange 26 na wszystkich trzech adsorbentach była silnie zależna od pH roztworu, natomiast siła jonowa roztworu nie wpływała na efektywność adsorpcji. Kinetyka adsorpcji była zgodna z modelem reakcji pseudo-drugiego rzędu. Etapem decydującym o szybkości adsorpcji jest dyfuzja barwnika w warstwie przypowierzchniowej. Proces adsorpcji równowagowej barwnika Direct Orange 26 na wszystkich badanych adsorbentach najlepiej opisuje izoterma Langmuira. Maksymalne zdolności adsorpcyjne dla torfu, węgla brunatnego i węgla kamiennego wynosiły odpowiednio 17,7, 15,1 i 13,8 mg/g. Wyniki wskazują, że torf, węgiel brunatny i węgiel kamienny mogą być rozważane jako alternatywne adsorbenty do usuwania barwników azowych z roztworów wodnych.